J Comput Electron (2012) 11:364–373
DOI 10.1007/s10825-012-0416-9

# Analysis and design of terahertz microstrip antenna on photonic bandgap material

**Kumud Ranjan Jha · G. Singh**

Published online: 3 August 2012


**Abstract** In this paper, a dielectric slab with periodic implantation of the air gaps has been analyzed. An effective dielectric permittivity of the 1-D photonic bandgap substrate material (PBG material) with host material as Polytetrafluoroethylene (PTFE) has been computed at 600 GHz. Based on the extracted effective dielectric permittivity, a rectangular microstrip patch antennas on thin and thick 2-D PBG material as substrate have been designed. The electrical performances of the antennas have been simulated by using two different simulators, CST Microwave Studio based on the finite integral technique and Ansoft HFSS based on the finite element method. This proposed antenna on the PBG material as substrate shows the significant enhancement in the directivity. To validate the homogenized medium approximation, the effect of the antenna position on the substrate material has been observed. The response of antenna has been found to be independent of its position. Various electrical parameters of the proposed antennas have been compared with reported literature. In addition to this, the operating frequency of one of the antenna has been scaled down by the factor of 50 and its various results have been compared with the results obtained at 600 GHz.

K.R. Jha
School of Electronics and Communication Engineering, Shri Mata Vaishno Devi University, Katra, Jammu and Kashmir, 182301, India
e-mail: jhakr@rediffmail.com

G. Singh (✉)
Department of Electronics and Communication Engineering, Jaypee University of Information Technology, Solan 173215, India
e-mail: drghanshyam.singh@yahoo.com

**Keywords** Terahertz spectrum · Electromagnetic band gap · Metamaterial · Microstrip patch antenna · Directivity · Radiation efficiency

## 1 Introduction

Terahertz regime of the electromagnetic spectrum extends from millimeter through micrometer in wavelength encompassing frequency approximately 0.1 to 10 THz. This band of electromagnetic spectrum finds a number of potential applications in various fields [1, 2]. In addition to these conventional applications, the terahertz wireless communication system is also being explored in detail [3, 4]. For an efficient communication in this band of the spectrum and to combat path losses, there is the requirement of highly directive antennas. In general, the terahertz radiators are designed using photomixer and photoconductive materials [5, 6]. However, these kind of the antennas suffer from poor directivity and reduced impedance bandwidth due to the high output impedance of the source and mismatch between the source and radiator [7–9]. In addition to this, the source power is also relatively low. To overcome this limitation, the high power integrated as well as discrete sources, efficient detectors and mixers are being developed [2, 4, 10, 11]. With the development of interconnects and passive radiators, these discrete devices can be integrated in the conventional source-interconnect-radiator-detector as a terahertz communication chain. Ultimately, it would be possible to realize a complete terahertz communication system with the development of interconnects and efficient radiators apart from sources and detectors. To meet the requirement of interconnects, waveguides and varieties of planar transmission line can be designed and implemented in the terahertz wireless communication system. The most versatile interconnect is a

waveguide, which can be used up to 1.0 THz [12]. Kadoya et al. [13] have investigated the microstrip lines and coplanar waveguides in the time domain at the terahertz frequency by using low dielectric permittivity substrate material both numerically as well as experimentally. They have also studied the propagation characteristics of the wave in this regime of the spectrum. Yeh et al. [14] have designed a terahertz ribbon type waveguide to convey the energy from one point to the other point and have shown the superiority of this device over the conventional microstrip-line.

It indicates that a microstrip antenna can be suitably integrated with sources and detectors and advantages of this kind of the antenna like low-cost, compatibility, and reliability can be harnessed for the terahertz wireless communication. However, the main drawback of the microstrip antenna is its poor directivity and the low gain at the microwave frequency [15]. At the terahertz frequency, to combat the path-loss, it is necessary to improve the directivity and gain of the antenna so that it could play a crucial role in the successful implementation of the wireless communication system. In the microwave frequency regime, various researchers have used high dielectric permittivity or thick substrate material [16–19] to improve the electrical performance of the microstrip antenna. However, the application of high dielectric permittivity material leads to shock wave at the air-substrate interface in the millimeter or terahertz regime of the spectrum [20]. Further, the application of thick substrate leads to surface wave loss due to the trapping of energy within the substrate [21] and reduction in the substrate thickness reduces the performance and mechanical strength of the antenna. To reduce the surface wave loss, either effective dielectric permittivity or thickness of material has to be reduced. To reduce the effective dielectric permittivity, the property of material is artificially altered with by using the periodic air-defects in the homogeneous host material. This heterogeneous material is called photonic bandgap material.

Earlier, various researchers [22–24] have used PBG material as the substrate to enhance the electric performance of microstrip antenna in the microwave frequency range. Recently, Singh et al. [25, 26] have proposed the rectangular microstrip patch antenna using PBG material as the substrate at terahertz frequency. Apart from this, the terahertz microstrip antennas on the thin and thick homogeneous substrate material have also been reported in [27–29]. The gain and radiation efficiency of these antennas are quite low and there is the lack of the analysis of PBG substrate material behavior. In general, the dielectric permittivity of the PBG materials is reduced which is used to enhance its electrical performance. However, the phenomenon of reduction of the effective dielectric permittivity of the PBG material using low relative dielectric permittivity substrate material as the host with the air-defects has not been discussed in the terahertz frequency regime.

In the present contribution, we have analyzed the effect of the periodic air-defects in the low dielectric permittivity 1-D and 2-D substrate material. Further, the work has been extended to find its suitable application as the substrate material to improve the electrical performance of the microstrip antenna in the terahertz spectrum. The organization of the paper is as follow. In Sect. 2, we have computed an effective dielectric permittivity of the PBG materials at 600 GHz. In Sect. 3, we have designed and simulated a patch antenna on the thin substrate to show the permittivity reduction phenomenon. In Sect. 4, we have designed an antenna on the thick substrate material and compared the performance of this antenna by using two different simulation techniques in Sect. 5. In Sect. 6, we have compared the electrical performance of the thick-substrate-antenna with the reported literature. In Sect. 7, the scaled down model of the antenna is presented. Finally, Sect. 8 concludes the work.

## 2 Analysis of photonic bandgap as substrate

In general, to reduce the refractive index of a material, metamaterials are used which have the negative dielectric permittivity, permeability, or both. To designs this kind of material, the conducting wires or split ring resonators are frequently used. However, the implantation of thin conducting wire in the microstructure homogeneous substrate at the terahertz frequency is relatively challenging task. To overcome this problem, in place of conducting wire, air-defects may be used to reduce the effective permittivity of the material. In this way, the PBG materials can be fabricated by using the techniques reported in [30, 31]. Recently, Lu and Prather [32] have studied the behavior of air-cylinder defect PBG materials and found that this kind of material can attain negative dielectric permittivity and magnetic permeability, simultaneously. It indicates that the refractive index of the homogeneous substrate can be reduced below 1.0 with the periodic implementation of the air-cylinders in it. The refractive index would depend on the lattice factor ($k$) of the defect material where $k$ is the ratio of radius of air cylinder ($r$) to the distance ($a$) between two air-cylinders. Since the dielectric permittivity of the substrate can be brought in the negative region, it may also be possible to control the dielectric permittivity to a value lesser than 1.0. In order to investigate this possibility, we present the front view of 1-D PBG material in Fig. 1. The host material of the PBG material is Polytetrafluoroethylene (PTFE) ($\varepsilon_r = 2.08$) whose length and width are 1000 μm and 100 μm, respectively. In the host material, cylindrical air defects of radius $r = 10$ μm and centre-to-centre inter-cylinder spacing $a = 100$ μm, have been used. The substrate thickness and the length of air cylinders are 200 μm.

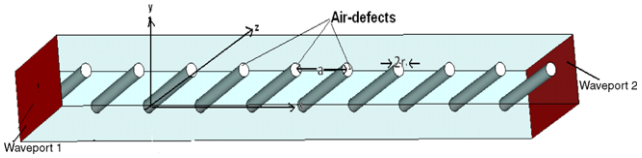


**Fig. 1** Perspective view of 1-D photonic bandgap

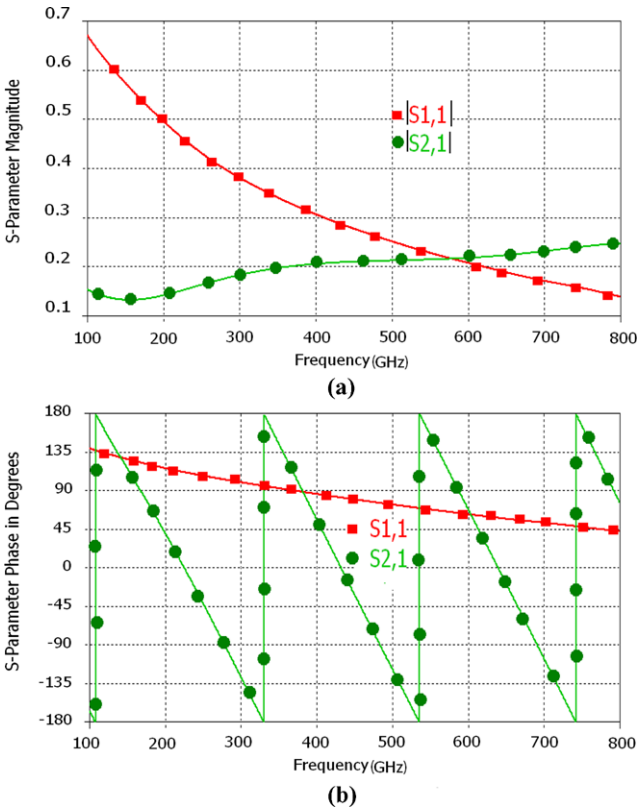


**Fig. 2** Simulated (**a**) magnitude and (**b**) phase of the scattering parameters of the 1-D PBG material slab

This structure is simulated by using the CST Microwave Studio with the following boundary condition. Top and bottom ($z$-axis) of PBG material is assigned with perfect electric conductor (PEC) where tangential component of electric field is zero ($E_t = 0$). Other four faces of the cuboids is assigned with the open boundary i.e. perfectly matched layer (PML). In other word, the structure is placed in the parallel plate waveguide. Two wave-ports with electric field oriented along the $z$-axis are placed at the left and right boundary (along $x$-axis). The magnitude and phase (degree) of the transmission and reflection coefficients of the proposed PBG materials at frequency range 100–800 GHz are shown in Fig. 2(a) and (b), respectively.

From Fig. 2(a), it is revealed that the structure opposes the transmission of the wave in this material. The magnitude of the $S_{21}$ parameter is always less than 0.22 in the simulated frequency range. We are interested to investigate an effective dielectric permittivity of this material near cross over the frequency of $S_{11}$ and $S_{21}$ parameter which is 600 GHz. At this frequency, the magnitude and phase of the scattering parameter is presented in Table 1. There are number of techniques to extract the effective dielectric permittivity and magnetic permeability of the metamaterials. Among them, an effective medium approach is quite efficient because it simplifies the sign ambiguity of the impedance, which is dependent on the transmission and reflection parameter of the material [33]. As per this technique, the effective dielectric permittivity and magnetic permeability are related to the refractive index and wave impedance as

$$\mu_{eff} = nz, \qquad \varepsilon_{eff} = n/z \tag{1}$$

where $\mu_{eff}, \varepsilon_{eff}, n$ and $z$ are the effective magnetic permeability, effective dielectric permittivity, refractive index and wave impedance, respectively. The wave impedance $z$ is related to scattering parameters as follow.

$$z = \pm\sqrt{\frac{(1+S_{11})^2 - S_{21}^2}{(1-S_{11})^2 - S_{21}^2}} \tag{2}$$

$$e^{jn\beta a} = \frac{S_{21}}{1 - S_{11}\frac{z-1}{z+1}} \tag{3}$$

where $z$ and $n$ are complex numbers. The solution of (3) may be written in the following form [33].

$$n = \frac{\mathrm{Im}\{\ln(e^{jn\beta a})\} + 2m\pi - j\,\mathrm{Re}\{\ln(e^{jn\beta a})\}}{\beta a} \tag{4}$$

However, to design an antenna on a substrate material, the knowledge of the real part of the effective dielectric permittivity ($\varepsilon_{eff}$) is required to obtain various geometric parameter of the antenna. The real part of the effective permittivity of the substrate is obtained by simplified Eq. (3) and resultant equation is shown (5).

$$jn\beta a = \ln\left(\frac{S_{21}}{1 - S_{11}\frac{z-1}{z+1}}\right) = x + jy \tag{5}$$

After separating real and imaginary part of (5), we get the value of $n$ equal to

$$n = \frac{y}{\beta a} \tag{6}$$

where $\beta$ and $a$ are the free space wave number and the inter-cylinder-spacing, respectively [34]. The value of real part of the effective permittivity ($\varepsilon'_{eff}$) can be easily determined and it may lie below 1.0 depending on the value of $n$ and $z'$. The extracted value of the wave impedance, refractive index and effective dielectric permittivity from Fig. 2 are shown in Table 1.

From Table 1, it is seen that the dielectric permittivity is less than 1.0 and it has been achieved for low-dielectric permittivity host material. Further, the value of the effective permittivity of the material may be varied by changing the lattice constant ($k$) [35].

**Table 1** Effective permittivity of pbg materials at 600 GHz

| $\varepsilon_r$ | $\lvert S_{11}\rvert$ | $\angle S_{11}$ (deg) | $\lvert S_{21}\rvert$ | $\angle S_{21}$ (deg) | $z$ | $n$ | $\varepsilon_{eff}$ |
|---|---|---|---|---|---|---|---|
| 2.08 | 0.208 | 62.52 | 0.218 | 69.17 | 1.17+j0.41 | 0.686 | 0.743 |

## 3 Design of rectangular microstrip antenna on thin substrate

In general, the relative dielectric permittivity of the material is independent to its thickness ($d$) for $d \ll \lambda_0$ [34]. Hence, we have designed a microstrip antenna on 50 μm thick substrate in this section using the value of effective dielectric permittivity of the material presented in Table 1 as substrate. Since the physical dimensions of the microstrip antenna are governed by the substrate permittivity, we have not considered the effect of the change in the relative magnetic permeability. However, the change in the relative magnetic permeability may contribute to the change in the surface wave efficiency of the microstrip antenna [36] and it can be investigated independently.

### 3.1 Antenna design on thin substrate

As we know, with the reduction in the effective dielectric permittivity of the material, the guided wavelength is increased. At the microwave frequency, the device dimension is in sub or multiple integer of the wavelength. Therefore, with the increased guided wavelength, the overall size of the circuit on the substrate is increased. However, at terahertz frequency where wavelength is quite small, the apparent longer wavelength reduces the fabrication complexity and increases the error tolerance. To see the effect of reduction in the effective dielectric permittivity of the material, we have designed a microstrip antenna on 2-D PBG material as substrate of dimension $1000 \times 1000$ μm$^2$ whose effective dielectric permittivity has been investigated and presented in Table 1. The radiating patch, feed-line and ground plane are made of copper of thickness 20 μm. Generally, in the microwave region, the patch dimensions for the positive dielectric permittivity materials are calculated using following formulas provided substrate thickness ($h$) $\ll$ free-space wavelength ($\lambda_0$) [37].

$$W = \frac{c}{2f_r}\sqrt{\frac{2}{\varepsilon_{eff}+1}} \tag{7}$$

In (7), $W$, $c$, $f_r$ and $\varepsilon_{eff}$ are the width of the radiating patch, velocity of the light, resonance frequency and effective permittivity of the substrate, respectively. In the present case the value of $W$ is equal to 267 μm. However, the suitable length of the radiating patch ($L$) has been obtained by the parametric study. The effect of the $L$ on the resonance frequency is shown in Fig. 3.

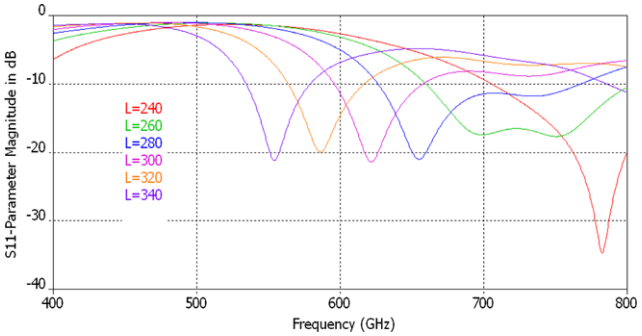


**Fig. 3** Effect of the length (in μm) of the antenna on the resonance frequency

In Fig. 3, the value of $L$ has been varied from 240 μm to 340 μm in the step of 20 μm. With the increase in the length of the radiating patch, the resonance frequency shifts downward. However, in all these conditions, the length of the radiating patch is always greater than the free-space half wavelength at the resonant frequency. In general, for the substrate with $\varepsilon_{eff} > 1$, the length of the resonator is calculated by using the following formula.

$$L = \frac{c}{2f_r\sqrt{\varepsilon_{eff}}} - 2\Delta l \tag{8}$$

where

$$\Delta l = 0.412h\frac{(\varepsilon_{eff}+0.3)(\frac{W}{h}+0.264)}{(\varepsilon_{eff}-0.258)(\frac{W}{h}+0.8)} \tag{9}$$

In the antenna design, the length of the radiating patch is kept less than the half of the free space wavelength i.e. $L < \lambda_0/2$ as the maximum length of the radiator in the free space is equal to $\lambda_0/2$. The value of $L$ is further reduced due to the use of the dielectric substrate and the fringing effect and it is inversely proportional to the square root of $\varepsilon_{eff}$ as shown in (8). From Fig. 3, it is seen that the patch length is always greater than $\lambda_0/2$ which indicates that this condition is met by using the concept of the reduced effective permittivity below 1.0. From this analysis, it is clearly revealed that the calculated value of $\varepsilon_{eff}$ and $\varepsilon$ for the 1-D substrate is less than 1.0.

### 3.2 Feeding mechanism

At terahertz frequency, the planar feeding technique is comparatively better choice against others due to the simplicity in the fabrication. However, the width of feed line is an important factor in antenna design to match the impedance. To achieve the better matching, contact feeding with narrow microstrip line has been used. The advantage of using narrow feed-line has been described in [38]. The length and width of the feed-line are 250 μm and 20 μm, respectively.

Based on the parametric study as discussed earlier, the value of $L$ has been optimized and it is equal to 308 μm.

**Table 2** Comparisons of the gain and directivity at 600 GHz

| Substrate | CST Microwave Studio | | Ansoft HFSS | | | |
|---|---|---|---|---|---|---|
| | | | Finite ground | | Infinite ground | |
| | Directivity (dBi) | Gain (dBi) | Directivity (dBi) | Gain (dBi) | Directivity (dBi) | Gain (dBi) |
| Homogeneous | 8.993 | 8.325 | 7.21 | 7.18 | 10.44 | 10.40 |
| PBG Material | 9.086 | 8.807 | 9.06 | 8.86 | 11.02 | 10.94 |

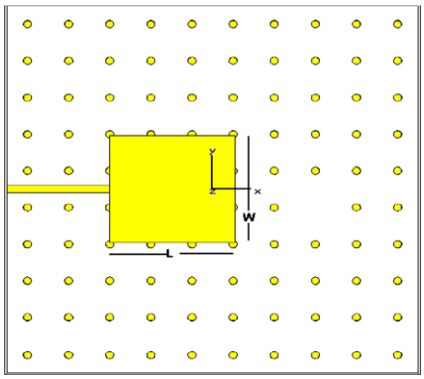


**Fig. 4** Schematic diagram of the proposed antenna

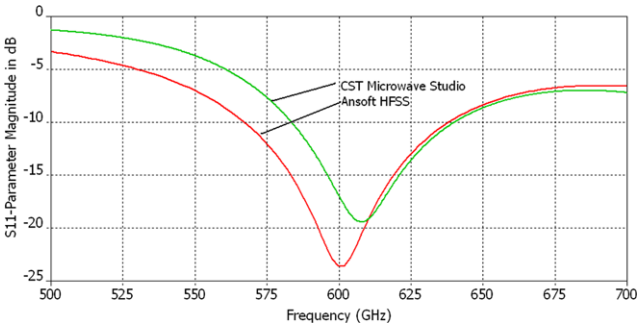


**Fig. 5** Reflection co-efficient (dB) of the proposed rectangular microstrip antenna on PBG material as substrate at terahertz frequency

However, the value of $W$ has been kept equal to 267 μm as calculated using (7). The antenna has been designed on the $1000 \times 1000\ \mu m^2$ 2-D substrate and ground plane size. Other parameters of the substrate are same as discussed in the previous section. The radiating patch, feed line and ground plane are made of copper of thickness 20 μm. The layout of the antenna is shown in Fig. 4.

The structure has been simulated in the 500–700 GHz band by using the CST Microwave Studio in the transient solver. To excite the antenna, the wave-port has been employed. The width and height of the port is equal to 200 and 120 μm, along $y$- and $z$-axis, respectively. The port is placed at $x_{min}$ position equal to −500 μm. To achieve the maximum accuracy, the adaptive mesh refinement radio button in the transient solver has been activated. To see the correctness of the analysis, we have re-simulated the structure by using Ansoft HFSS, another commercial simulator with the wave-port and resonance occurs at 600 GHz. The $S_{11}$-parameter (dB) of the antenna is shown in Fig. 5. From this figure, it is seen that the resonance condition of the antenna is satisfied by the selected value of $W$ and $L$ in the both simulation environment.

The −10 dB impedance bandwidth of the antenna is 12 % and 10.6 % in the case of Ansoft HFSS and the CST Microwave Studio, respectively. To compare the directivity and gain of the proposed antenna, we have replaced the PBG substrate material by a homogeneous substrate of relative dielectric permittivity 2.08 (host material) while keeping other parameters constant and simulated the structure by using these two simulators. Comparison of the directivity and gain is shown in Table 2.

Table 2 indicates that the gain is marginally increased with the implementation of PBG crystal in comparison to the homogeneous substrate. In the case of Ansoft HFSS simulation, we have considered finite as well as infinite ground planes and the result on the infinite ground is fairly good. The directivity of the antenna can be further improved by optimizing the lattice constant ($k$).

### 3.3 Effect of lattice constant of PBG substrate material on the electrical parameter of the antenna

In the above analysis, we have used the PBG material of square lattice where the radius of the air cylinder $r$ is 10 μm and distance between two cylinders $a$ is 100 μm. In this way, the lattice factor ($k$) is equal to 0.1. The lattice factor can be used as an additional tuning parameter to improve the performance of the antenna. We have used this parameter to enhance the gain and the directivity of the proposed antenna. The radius of the air cylinder has been varied from 0.0 to 45.0 μm in the step of 5.0 μm and improvement in the directivity has been observed which is shown in Fig. 6.

From Fig. 6, it is seen that with the increase in the lattice factor up to $k = 0.25$, the directivity increases and there after it reduces and for $k = 0.40$, the directivity is 8.80 dBi which is below the directivity obtained with the homogenous substrate as shown in Table 2. Here, it is important to note that with the increase in the value of $k$, the volume of the air-defects in the substrate is being increased. With the

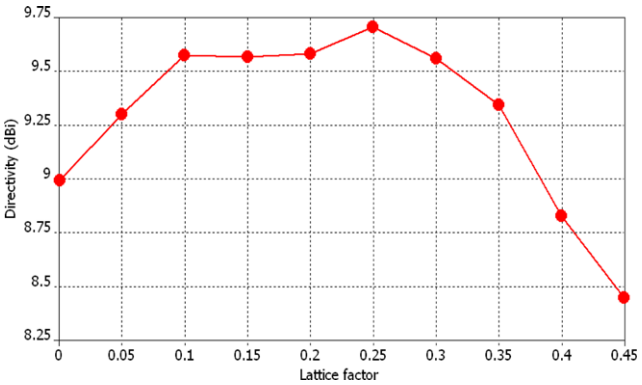


**Fig. 6** Effect of the variation in $k$ on the directivity of the proposed antenna at 600 GHz

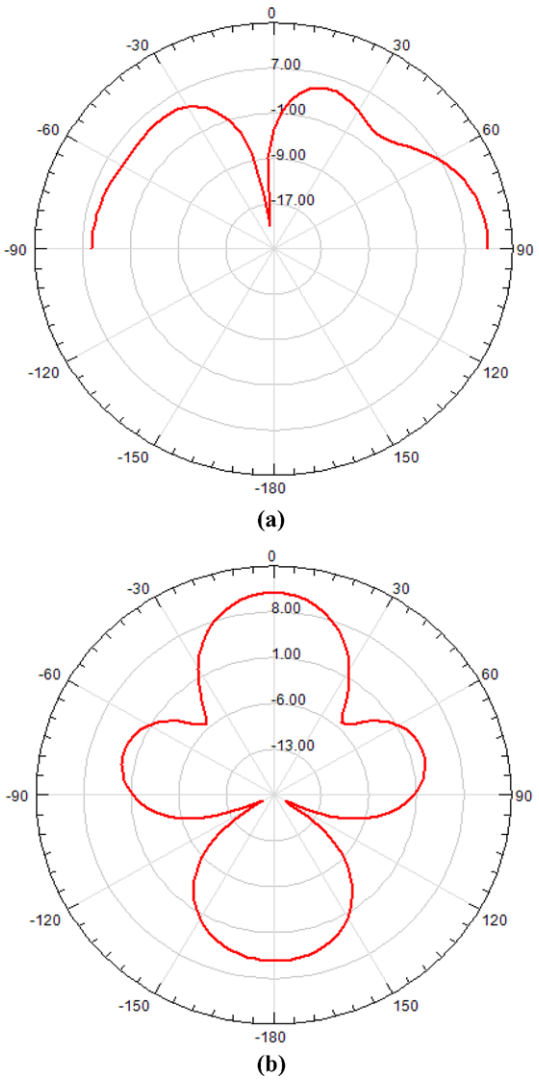


**Fig. 7** Radiation pattern of the proposed antenna in (**a**) $xz$ plane and (**b**) $xy$ plane

increase in $k$, the directivity must either increase or decrease in the monotonous way. However, after $k = 0.25$, the directivity starts falling in spite of the increase in the volume of

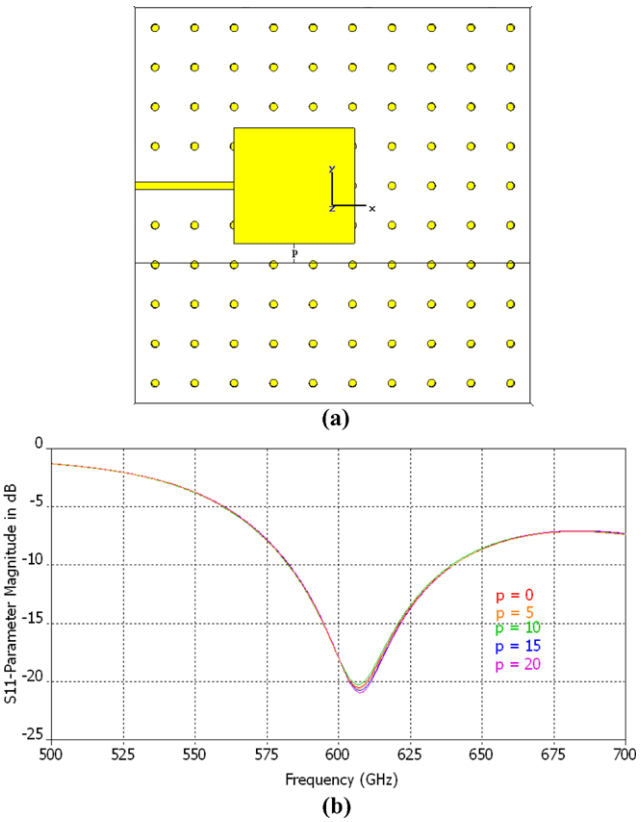


**Fig. 8** Proposed antenna with (**a**) shift in position ($p$ in μm) and (**b**) its effect on $S_{11}$ parameter (dB)

the air-defects and it indicates that first of all the dielectric permittivity of the material is reduced below 1.0 and then it tends towards the permittivity of vacuum.

To meet the bandwidth criteria and resonance frequency, a trade-off between $k$ and directivity can be made. However, in our design, we have kept this value equal to $k = 0.1$ only. The directivity radiation pattern of this antenna obtained by using the Ansoft HFSS for $k = 0.1$ is shown in Fig. 7 in $xz$ and $xy$-plane. The radiation pattern of this antenna is maximum at the $\theta = 90°$ and $\phi = 0°$ and the maximum directivity is 11.02 dBi.

### 3.4 Effect of the antenna position on the electrical performances

To analyze the effect of the antenna position on the finite size ($4\lambda_0^2$ μm$^2$) substrate material and ground plane, the position of the feed line and radiating patch has been shifted from its original position. The position of the radiating patch of the antenna shown in Fig. 4, has been shifted by a variable $p$ along $y$-axis and it is shown in Fig. 8(a). For three different values of $p$, the $S_{11}$ parameter has been obtained by simulating the structure in the CST Microwave Studio which is shown in Fig. 8(b). From Fig. 8(b), it is revealed that there is maximum 0.5 dB variation in the $S_{11}$ parameter at

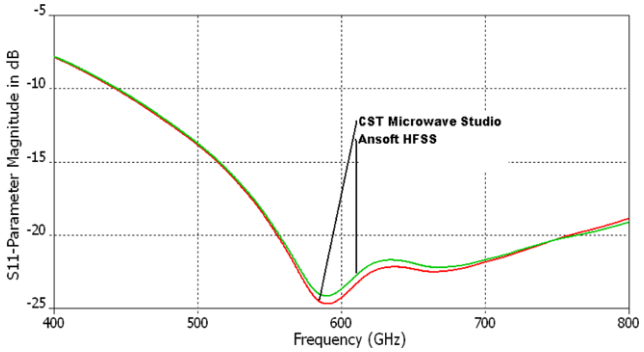


**Fig. 9** Simulated reflection co-efficient (dB) on the thick substrate antenna

the 500–700 GHz frequency range. Moreover, the resonance frequency converges in all these cases near 600 GHz. The result obtained in this case is similar to the result presented in Fig. 5 achieved by the same simulator. Apart from this, the directivity of the antenna is also consistent and is equal to 9.08 dBi as mentioned in Table 2. In this way, we conclude that the homogenized medium approximation is validated.

## 4 Antenna design on relatively thick substrate

In the previous section, we have discussed the possibility of the use of the reduced effective dielectric permittivity substrate in antenna design on the thin substrate. However, the main objective is to increase the antenna's directivity to compensate the loss of energy in the terahertz spectrum. In general, the electromagnetic energy is trapped in the thick substrate and it causes the surface wave loss. To overcome this problem, the relatively thicker PBG material substrate may be the better choice. In order to investigate this effect, we have considered a microstrip patch antenna on the substrate thickness of 200 μm. In this case, all geometrical parameters of the antenna structure except the substrate thickness is unchanged. The substrate thickness of the antenna has been increased to 200 μm. The reflection co-efficient of the antenna in this case is shown in Fig. 9.

To simulate this structure, the mesh cells have been increased to 1358265 by increasing the number of lines per wavelength equal to 30 in the mesh density control and using adaptive mesh refinement in the CST Microwave Studio. To check the correctness of the analysis, the structure has also been re-simulated using Ansoft HFSS. The reflection co-efficient (in dB) obtained by these simulations are shown in Fig. 9. The structure shows the resonance near 600 GHz. However, the antenna can support a wide −10 dB impedance bandwidth. The wide impedance bandwidth is attributed to the increase in the substrate thickness.

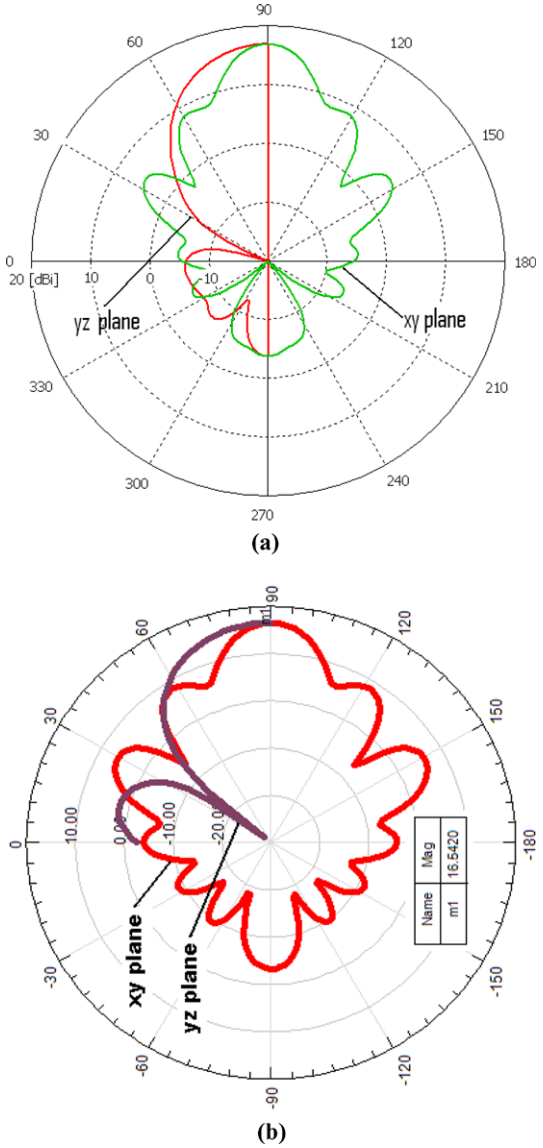


**Fig. 10** Radiation pattern of the proposed antenna on thick substrate at 600 GHz obtained by using (**a**) CST Microwave Studio and (**b**) Ansoft HFSS

## 5 Comparison of radiation pattern of the antenna on the thick substrate

To check the correctness of the analysis of the antenna on the thick substrate material, the directivity of the proposed antenna on the thick substrate has been obtained by simulating the structure by two different simulation techniques and the results are convergent in these cases. The radiation pattern of the structure obtained by CST Microwave Studio and Ansoft HFSS are presented in Fig. 10(a) and (b), respectively.

The directivity of the proposed antenna obtained by using CST Microwave Studio and Ansoft HFSS are 16.99 dBi and 16.542 dBi, respectively. Only a variation of 0.448 dBi

**Table 3** Comparison of electrical performance with Yagi–Uda type antenna

| Frequency (GHz) | Proposed antennas | | | | Ref. [29] | |
|---|---|---|---|---|---|---|
| | Substrate thickness (50 μm) | | Substrate thickness (200 μm) | | Substrate thickness (300 μm with 296 μm cut in substrate) | |
| | Direct. (dBi) | Rad. efficiency (%) | Direct. (dBi) | Rad. efficiency (%) | Direct. (dBi) | Rad. efficiency (%) |
| 590 | 9.799 | 93.62 | 17.02 | 88.17 | 10.9 | 80.8 |
| 636 | 8.175 | 93.92 | 17.14 | 89.14 | 10.9 | 80.1 |

has been noticed between these two simulations. The radiation efficiency and gain of the proposed antenna are about 87.91 % and 16.43 dBi, respectively. The half power beamwidth of the proposed antenna in $xy$ and $yz$ plane is 21.7° and 21.4°, respectively.

## 6 Comparison of results

We have compared the performance of the proposed antenna with various reported literature which have been obtained by using the CST Microwave Studio Simulation. Initially, we have compared the performance of the proposed antenna with respect to the Yagi–Uda type antenna [29] which has been designed on a high dielectric permittivity substrate material of overall thickness 300 μm with the removal of 296 μm thick substrate beneath the antenna structure. However, the overall surface area of the antenna is quite large. Comparison of various electrical parameters is presented in Table 3.

Finally, the electrical performance of the proposed antenna on the thick substrate has also been compared with the electrical performance of photonic crystal substrate antenna [26]. In this work, the antenna has been designed on the high permittivity substrate material of the same thickness and lattice factor. It is interesting to note that, the patch and feed size of the antenna reported in that work is quite larger than the proposed antenna in this manuscript. Due to this reason, performance of the antenna is inferior to the present structure. In order to show the superiority of proposed antenna, we have compared the directivity, gain and radiation efficiency at 693.45 GHz. The computed gain and directivity of the proposed antenna at 693.45 GHz are equal to 16.99 dBi and 17.33 dBi in comparison to 4.50 dBi and 6.239 dBi reported in [26], respectively. In addition to this, the proposed structure shows the directivity and gain equal to 16.94 dBi and 17.23 dBi, respectively at 740.8 GHz which is quite better than the reported work in [25, 28].

## 7 Scaled down model of the proposed antenna

The microwave frequency is scalable. When the operating frequency is decreased by constant factor, the thickness of the substrate must be increased by the same factor. In order to meet this requirement, the operating frequency of the proposed antenna on 50 μm thick substrate as shown in Fig. 8(a) with $p = 0$, has been scaled down by the factor of 50. To scale down this model, the geometric parameters of the antenna except the thickness of copper have been multiplied by a factor of 50. The thickness of copper clad has been kept equal to 20 μm as mentioned earlier. Since the commercial copper clad substrates are found to have the metallization in the order of micrometer so we have not changed this value while scaling down the frequency. At microwave frequency regime, the accuracy of the numerical analysis techniques: (a) CST Microwave Studio and (b) Ansoft HFSS are already proven. In other word, the similarity of various responses of the scaled down model with the result of high frequency responses as shown in Fig. 5 and Fig. 7 would prove the correctness of analysis technique and results. To analyze this effect, we have simulated the scaled down structure in the 8–16 GHz range by using Ansoft HFSS simulator. The $S_{11}$ parameter response of the model is shown in Fig. 11.

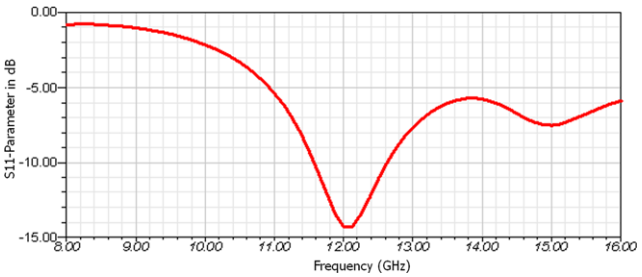


**Fig. 11** $S_{11}$ parameter (dB) of the scaled down model of the proposed antenna

From Fig. 11, it is seen that the resonance of the antenna occurs near 12 GHz. The scattering parameter pattern of the scaled model of the antenna is similar to the pattern obtained at high frequency by the same simulation technique which is presented in Fig. 5, except a shift in the magnitude of $S_{11}$ parameter by 6 dB at the resonance frequency. This deviation is attributed to the metallization thickness as we have not scaled up this value and kept it equal to 20 μm only. The −10 dB fractional bandwidth of the antenna at 12 GHz centre frequency is equal to approximately 10 % a comparable value of 12 % at 600 GHz. The directivity radiation pattern

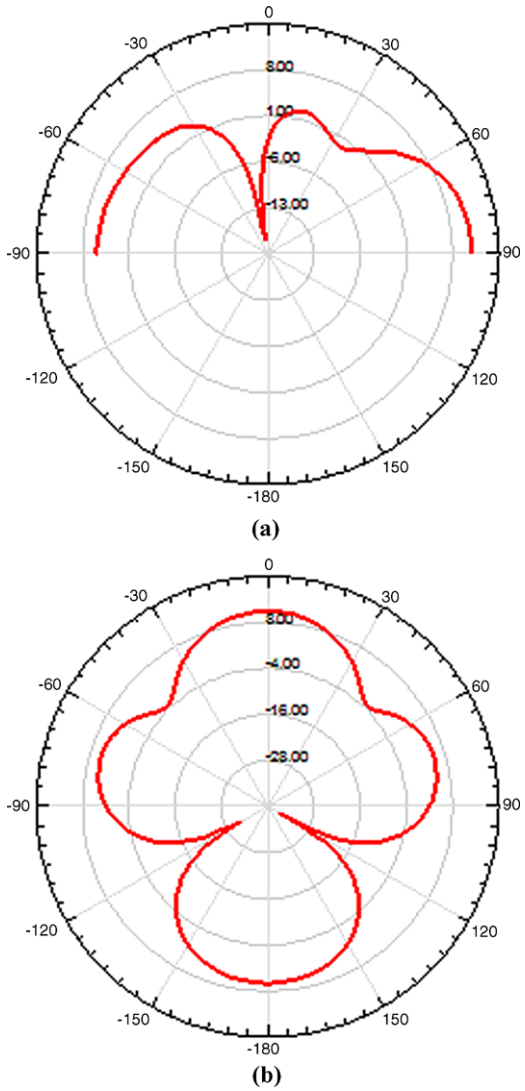


**Fig. 12** Radiation pattern of the scaled down antenna at 12 GHz in (**a**) $xz$ plane and (**b**) $xy$ plane

of the antenna in $xz$ and $xy$ plane at 12 GHz is shown in Fig. 12. From Figs. 12(a) and (b), it is seen that the radiation pattern at 12 GHz is similar to that of at 600 GHz as shown in Figs. 7(a) and (b). In addition to this, the directivity of the scaled down antenna at 12 GHz is about 10.92 dBi against the 11.02 dBi at 600 GHz mentioned in Table 2.

## 8 Conclusion

In this paper, a 1-D PBG material as substrate of the microstrip antenna at terahertz frequency has been analyzed. A method to calculate an effective dielectric permittivity of the PBG substrate material and its application in the antenna design has been proposed. Based on our predicted value of the effective dielectric permittivity, we have successfully designed two microstrip patch antennas on 2-D substrate material with different substrate thickness. Designed antennas show a good agreement in terms of resonance frequency. It verifies the dimension independent property of the extracted permittivity of the substrate material. The directivity of the proposed antenna is quite high to make it suitable for the application in the terahertz communication system. To check the correctness of the analysis, various parameters have been coherently simulated by using two different simulation techniques which are in the good agreement. In order to show the advantage of proposed technique and antenna, we have compared various electrical parameters with reported literature. In addition to this, we have scaled down the antenna's operating frequency by 50 and compared its performance with the high frequency response. The analysis will be extended to other materials and antenna topologies.

**Acknowledgements** The authors are sincerely thankful to the unanimous reviewers for their critical comments and suggestions to improve the quality of the manuscript.

## References

1. Siegel, P.H.: THz instruments for space. IEEE Trans. Antennas Propag. **55**(11), 2957–2965 (2007)
2. Williams, G.P.: Filling the THz gap–high power sources and applications. Rep. Prog. Phys. **69**(2), 301–306 (2006)
3. Piesiewicz, R., Jacob, M., Koach, M., Schoebel, J., Kuner, T.: Performance analysis of future multigigabit wireless communication systems and THz frequency with highly directive antennas in indoor environments. IEEE J. Sel. Top. Quantum Electron. **14**(2), 421–430 (2008)
4. Fitch, M.J., Ostiander, R.: Terahertz waves for communications and sensing. John Hopkins APL Tech. Dig. **25**(4), 348–355 (2004)
5. Brown, E.R., McIntosh, K.A., Nichols, K.B., Dennis, C.L.: Photo mixing upto 3.8 THz in low temperature grown GaAs. Appl. Phys. Lett. **66**, 285–287 (1995)
6. Verghese, S., McIntosh, K.A., Brown, E.R.: Optical and terahertz power limits in the low temperature GaAs photomixer. Appl. Phys. Lett. **71**, 2743–2745 (1997)
7. Matsuura, M., Tani, M., Sakai, K.: Generation of coherent terahertz radiation by photomixing in dipole photoconductive antennas. Appl. Phys. Lett. **70**, 559–561 (1997)
8. Gregory, I.G., Tribe, W.R., Cole, B.E., Evans, M.J., Linfield, E.H., Davies, A.G., Missons, M.: Resonant dipole antennas for continuous wave terahertz photomixers. Appl. Phys. Lett. **8**, 1622–1624 (2004)
9. Mendis, R., Sydlo, C., Sigmund, J., Feiginov, M., Meissnev, P., Hastnagel, H.L.: Spectral characterization of broadband THz antennas by photoconductive mixing: towards optimal antenna design. IEEE Antennas Wirel. Propag. Lett. **4**, 85–88 (2005)
10. Carr, G.L., Martin, M.C., Mckinney, W.R., Jordan, K., Neil, G.R., Williams, G.P.: Very high power THz radiation sources. J. Biol. Phys. **29**(2–3), 319–325 (2003)
11. Gallerano, G.P., Biedron, S.: Overview of terahertz radiation sources. In: Proc. Free Electron Laser Conf, Trieste, Italy, Aug. 29–Sep. 03, 2004, pp. 216–221 (2004)
12. Raisanen, A.V., Lehto, A.: Radio Engineering for Wireless Communication and Sensor Applications. Artech House, Boston (2003)
13. Kadoya, Y., Onuma, M., Yanagi, S., Ohkubo, T., Sato, N., Kitagawa, J.: THz wave propagation on strip lines: devices, properties and applications. Radioengineering **17**(2), 48–55 (2008)

14. Yeh, C., Shimabukuro, F., Siegel, P.H.: Low-loss terahertz ribbon waveguides. Appl. Opt. **44**(28), 5937–5946 (2005)
15. Bahl, I.J., Bhartia, P.: Microstrip Antennas. Artech House, Dedham (1980)
16. Nishiyama, E., Aikawa, M.: FDTD analysis of stacked microstrip antenna with high gain. Prog. Electromagn. Res. **33**, 29–43 (2001)
17. Yang, G.M., Jin, R.H., Xiao, G.B., Vittoria, C., Harris, V.G., Sun, N.X.: Ultra wideband (UWB) antennas with multi-resonant split-ring loops. IEEE Trans. Antennas Propag. **57**(1), 256–260 (2009)
18. Nishiyama, E., Aikawa, M., Egashira, S.: Stacked microstrip antenna for wideband and high gain. IEE Proc., H Microw. Antennas Propag. **151**(2), 143–148 (2004)
19. Kishk, A.A., Shafai, L.: Gain enhancement of antennas over finite ground plane covered by a dielectric sheet. IEE Proc., H Microw. Antennas Propag. **134**(Pt. 1 H), 60–64 (1987)
20. Grischkowsky, D., Duling, I.N. III, Chen, T.C., Chi, C.-C.: Electromagnetic shock waves from transmission lines. Phys. Rev. Lett. **59**(15), 1663–1666 (1987)
21. Bhattacharyya, A.K.: Characteristics of space and surface waves in a multilayered structure. IEEE Trans. Antennas Propag. **38**(8), 1231–1238 (1990)
22. Yang, H.Y.D., Alexopoulos, N.G., Yablonovitch, E.: Photonic band-gap materials for high-gain printed antennas. IEEE Trans. Antennas Propag. **45**(1), 185–187 (1997)
23. Boutayeb, H., Denidni, T.A.: Gain enhancement of microstrip patch antenna using a cylindrical electromagnetic crystal. IEEE Trans. Antennas Propag. **55**(11), 3140–3144 (2007)
24. Park, Y.J., Herschlein, A., Wiesbech, W.: A photonic band-gap structure for guiding and suppressing surface waves in millimeter-wave antennas. IEEE Trans. Microw. Theory Tech. **49**(10), 1854–1859 (2001)
25. Sharma, A., Singh, G., Chauhan, D.S.: Design considerations to improve the performance of a rectangular microstrip patch antenna at THz frequency. In: Proc. 33rd International Conference on Infrared, Millimeter, and Terahertz Waves (IRMMW-THz 2008), USA, 15–19th Sept. 2008, pp. 1–2 (2008)
26. Singh, G.: Design consideration for rectangular microstrip patch antenna on electromagnetic crystal substrate at terahertz frequency. Infrared Phys. Technol. **53**(1), 17–22 (2010)
27. Jha, K.R., Singh, G.: Dual-band rectangular microstrip patch antenna at terahertz frequency for surveillance system. J. Comput. Electron. **9**(1), 31–41 (2010)
28. Sharma, A., Singh, G.: Rectangular microstrip patch antenna design at THz frequency for short distance wireless communication systems. J. Infrared Millim. Terahertz Waves **30**(1), 1–7 (2009)
29. Han, K., Nguyen, T.K., Park, I., Han, H.: Terahertz Yagi-Uda antenna for high input resistance. J. Infrared Millim. Terahertz Waves **31**(4), 441–454 (2010)
30. Munemassa, Y., Mitra, M., Takanao, T., Sano, M.: Lightwave antenna with a small aperture manufactured using MEMS processing technology. IEEE Trans. Antennas Propag. **55**(11), 3046–3051 (2007)
31. Lubecke, V., Mizuno, K., Rebeiz, G.: Micromachining for terahertz applications. IEEE Trans. Microw. Theory Tech. **46**(11), 1821–1831 (1998)
32. Lu, Z., Prather, D.W.: Calculation of effective permittivity, permeability, and surface impedance of negative-refractive photonic crystals. Opt. Express **15**(13), 8340–8345 (2007)
33. Kim, D., Choi, J.I.: Analysis of a high gain Fabry-Perot cavity antenna with an FSS superstrate: effective medium approach. Progress Electromagn. Res. Lett. **7**, 59–68 (2009)
34. Jha, K.R., Singh, G.: Analysis and design of enhanced directivity microstrip antenna at terahertz frequency by using electromagnetic bandgap material. Int. J. Numer. Model. **24**(5), 410–424 (2011)
35. Mosallaei, H., Samii, Y.R.: Periodic bandgap and effective dielectric materials in electromagnetics: characterization and applications in nanocavities and waveguides. IEEE Trans. Antennas Propag. **51**(3), 549–563 (2003)
36. Milligan, T.A.: Modern Antenna Design. IEEE Press, New York (2005)
37. Balanis, C.A.: Antenna Theory Analysis and Design. Wiley, New York (2001)
38. Dejean, G.R., Tentzeris, M.M.: A new high-gain microstrip Yagi array antenna with a high front-to-black (F/B) ratio for WLAN and millimeter-wave applications. IEEE Trans. Antennas Propag. **55**(2), 298–304 (2007)